A THEORETICAL MODEL FOR PREDICTING ALUMINUM OXIDE PARTICLE SIZE DISTRIBUTIONS IN ROCKET EXHAUSTS

by

Harvey L. Fein

Atlantic Research Corporation

Alexandria, Virginia

This work was performed for the Jet Propulsion Laboratory, California Institute of Technology, sponsored by the National Aeronautics and Space Administration under Contract NAS7-100.

ABSTRACT

The model is derived to describe the oxide particle size distribution obtained from internal burning, cylindrically perforated, aluminized, solid propellant grains. Particle growth is assumed to occur by diffusion of gaseous aluminum and aluminum oxides to the particle surface followed by a heterogeneous reaction to form condensed oxide, the overall rate being proportional to a concentration driving force and the particle area. The particle nucleation rate is assumed constant. Excellent agreement is obtained between experimental particle size distributions and the distributions predicted by the model. This agreement implies that the distribution is independent of chamber length and possibly chamber diameter, and depends upon only one arbitrary parameter characteristic of the nucleation rate. In terms of the number average particle volume, V_n, the normalized frequency, $f(v)$, for the distribution is given by:

$$f(v) = \frac{2}{V_n^{1/3}(6v)^{2/3}} \exp\left[-(6v/V_n)^{1/3}\right]$$

Further conclusions are that oxide condensation progresses to equilibrium in the chamber and that the nucleation mechanism is not homogeneous for aluminized propellants.

I. INTRODUCTION

Many advanced solid propellant formulations contain metals which yield condensed oxide particles as products of combustion. Although the theoretical performance of these propellants is generally superior to that of non-metalized formulations, the specific impulse efficiency of metalized formulations may be seriously reduced by the presence of these condensed products in the exhaust. This reduction in specific impulse efficiency

is generally attributed to the lack of interphase thermal and momentum equilibrium between the oxide particles and the gas phase and to the increased heat losses to the rocket hardware resulting from radiation by the particles. Thus, from engineering considerations alone, it is desirable to have a workable model which will allow the prediction of the particle size distribution of the oxide particles. This information is required to calculate the specific impulse inefficiencies associated with the presence of the particles in the rocket exhaust and thus to predict, in the design stage, the actual performance which might be realized from a specific rocket. Therefore, for the specific purposes of predicting the particle size distribution of aluminum oxide in rocket exhausts and gaining insight into the mechanism by which these particles are formed, the theoretical model which is the subject of this paper has been derived.

II. DERIVATION AND DISCUSSION OF THE MODEL

A. DESCRIPTION OF THE SYSTEM AND ASSUMPTIONS

The specific physical geometry for which the model is derived is that of a rocket chamber consisting of a cylindrically perforated, aluminized, solid propellant grain. A schematic diagram of this system is pictured in Figure 1. The arrows in the figure represent the flow of combustion products from the burning surface to the main stream and down the chamber length. Complete radial mixing is assumed throughout the chamber except within a thin low temperature region immediately adjacent to the propellant surface. In the main gas stream, plug flow (no axial mixing) of combustion products is assumed to prevail from the head end of the chamber ($x = 0$) to the nozzle entrance ($x = L$). Steady state is also assumed to prevail and the pressure and temperature are assumed constant throughout the main gas stream.

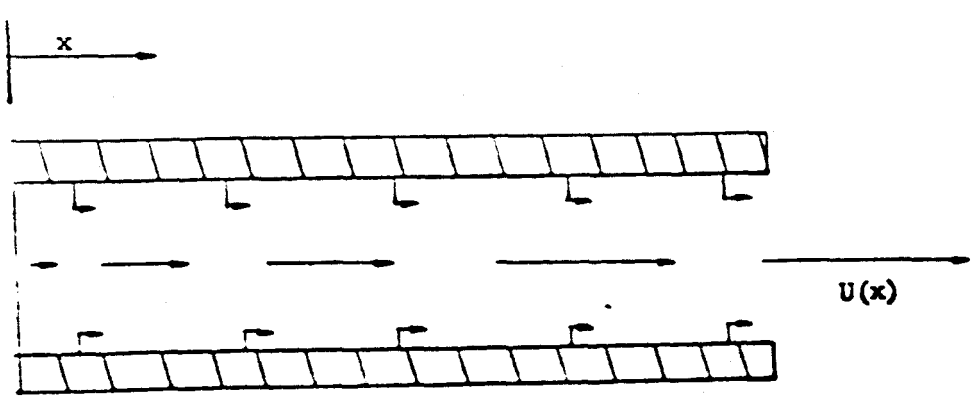

Figure 1. Schematic Diagram of a Burning Grain

Due to the increase in burning surface area with increasing x, the gas velocity past any x plane must increase with increasing x. It is assumed that the propellant burning rate does not vary with x (no errosive burning), that the decrease in the moles of gas from condensation of the oxide is small compared to the total moles of gas, and that the chamber diameter does not change significantly with time. Thus, the velocity of the combustion products is directly proportional to x and given by Equation (1):

$$U = N\rho_p r \cdot \frac{\pi d}{A} \cdot \frac{RT}{P} \cdot x \qquad (1)$$

where: U = velocity of combustion products (cm/sec)

N = moles of gas introduced into the chamber upon burning 1 gm of propellant, assuming thermodynamic equilibrium in the chamber (gm-moles/gm propellant)

ρ_p = solid propellant density (gm/cm^3)

r = linear burning rate of propellant (cm/sec)

d = chamber or port diameter (cm)

A = chamber or port cross sectional area (cm^2)

R = universal gas constant = 82.057 cc-atm/°K, gm-mole

T = chamber temperature (°K)

P = chamber pressure (atm)

It is assumed that preformed nuclei are introduced into the main gas stream at the constant rate of n_o nuclei per sec per cm of chamber length. Therefore, the total number of particles passing any given x plane, n_t, is given by:

$$n_t = n_o x \qquad (2)$$

The initial volume of a nucleus is assumed to be constant and is designated by v_o(cm^3).

Finally, some assumption must be made concerning the rate of growth of an oxide particle. The assumption made here is that the rate of growth of a particle, $dv/d\theta$, is given by the simple mass transfer law:

$$\frac{dv}{d\theta} = \frac{\gamma (C-C_e)\, \alpha M}{\rho} \qquad (3)$$

where: γ = an empirical rate constant which will be referred to as the growth constant (cm/sec)

C = concentration of the oxide in the gas phase (moles/cc)

C_e = equilibrium concentration of the oxide in the gas phase at the chamber temperature and pressure (moles/cc)

α = surface area of a single particle assuming that the particles are spherical (cm^2)

v = volume of a single particle (cm^3)

M = molecular weight of the oxide (gm/gm-mole)

ρ = density of the oxide in the condensed state (gm/cm^3)

θ = time (sec)

The formulation given by equation (3) is a general rate expression for a gas-film-controlled mass transfer process where a mobile species is transferred across a thin film adjacent to a surface α. It is implied by the definitions of C and C_e that we are concerned with a single molecular species, which has a gas phase concentration of C_e at the particle surface, α, and a concentration of C on the bulk stream side of the film. However, for the case of an aluminized propellant, the oxide, Al_2O_3, does not exist in the gas phase. Any aluminum in the gas phase exists as Al, AlO, Al_2O and Al_2O_2 as well as the aluminum oxidation products of other oxidizing elements, such as Cl, which may be present in the propellant. Thus, in the present case, the growth law of equation (3) must be interpreted as representing the rate of mass transfer of any or all of the lower oxides to the particle surface followed by a heterogeneous chemical reaction at the surface to produce liquid Al_2O_3. The possibility of particle growth by heterogeneous chemical reaction is documented in the review papers of Markstein* and Christensen, Knipe, and Gordon**.

---

* Markstein, George H., AIAA J., 1, 550, (1963)

** Christensen, H. C., R. H. Knipe, and Alvin S. Gordon, Survey of Aluminum Particle Combustion, Presented at the Meeting of the Western States Section of the Combustion Institute, University of Utah, Salt Lake City, 26 and 27 October 1964.

With the above interpretation of the particle growth law, C and C_e become fictitious quantities. Their computation will be discussed later in connection with the comparison of the model to experimental data. Furthermore, the above discussion notwithstanding, C and C_e will still be referred to for convenience as concentrations of the gaseous oxide. All of the assumptions necessary for the development of the model have not been set forth.

B. DERIVATION OF MODEL EQUATIONS

The first equation to be derived is the differential mass balance of the gaseous oxide taken over the main gas stream. Consider the small differential element of chamber length pictured in Figure 2. The rate of flow of gaseous moles of oxide

Figure 2. Differential Element of Chamber Length

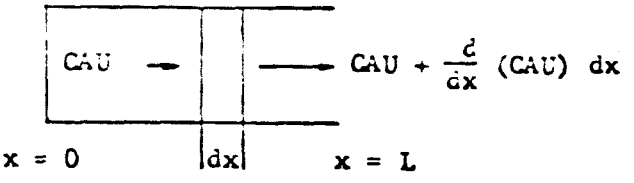

into this element from the main gas stream is CAU moles/second. The outflow of gaseous oxide to the main gas stream is CAU + $\frac{d}{dx}$ (CAU) dx moles/sec. Define C_i (moles/cc) as the initial concentration (before any condensation) of the oxide in the gas stream leaving the low temperature gas film adjacent to the propellant surface. Then the flow of condensable gaseous oxide into the differential element from the propellant surface is given by:

$$C_i N \pi \, dp_p \, r \, \frac{RT}{P} \, dx$$

moles/second.

Now, define a_t as the total surface area of all particles passing position x per second. Then, the total particle surface area per cc of chamber volume at position x is a_t/AU, and the total surface area of all particles in the differential element is $a_t dx/U$. Then from equation (3), the total moles of oxide that condenses in the differential element in one second is given by:

$$\gamma (C - C_e) a_t \, \frac{dx}{U}$$

Now, referring to the gaseous oxide, the sum of the flows into the differential element from the main gas stream and from the gas film adjacent to the propellant surface minus the flow out from the element to the main gas stream must equal the amount that condenses, or stated mathematically:

$$CAU + C_i N\bar{\pi} d\rho_p r \frac{RT}{P} dx - \left[CAU + \frac{d}{dx}(CAU)dx\right] = \gamma(C-C_e)a_t \frac{dx}{U} \tag{4}$$

Expanding equation (4) and eliminating U by means of equation (1) yields:

$$\frac{C_i N\bar{\pi} d\rho_p rRT}{P} - \frac{N\bar{\pi} d\rho_p rRTx}{P}\frac{dC}{dx} - \frac{CN\bar{\pi} d\rho_p rRT}{P} = \frac{\gamma(C-C_e)a_t AP}{N\bar{\pi} d\rho_p rRTx} \tag{5}$$

Define the accomplishment factor Φ by:

$$\Phi = \frac{C_i - C}{C_i - C_e} \tag{6}$$

and also define the maximum driving force, δ, by:

$$\delta = C_i - C_e \tag{7}$$

Then, changing the dependent variable in equation (5) from C to Φ and rearranging with the use of equation (7) yields:

$$\frac{d}{dx}(x\Phi) + \frac{Fa_t(\Phi-1)}{x} = 0 \tag{8}$$

where:

$$F = \frac{\gamma}{4\bar{\pi}}\left(\frac{P}{N\rho_p rRT}\right)^2 \tag{9}$$

Equation (8) is the simplest form of the differential equation describing the mass balance for the gaseous oxide taken around a differential element of the chamber. It now remains to formulate a_t as a function of x and Φ and then to find a solution to equation (8). Once this is accomplished, particle size distributions will be readily calculable in terms of the parameters of the model.

Let v_i equal the volume (cc) at x of a particle that was introduced into the main gas stream at $x = x_i$, and let α_i equal the surface area (cm^2) of this particle. Note that v_i and α_i are functions of both x_i and x, and are respectively equal to v_o and α_o at $x = x_i$. Since the particles are assumed to be spheres:

$$v_i = \frac{\pi}{6}\left(\frac{\alpha_i}{\pi}\right)^{3/2} \tag{10}$$

and thus:

$$dv_i = \frac{1}{4}\sqrt{\frac{\alpha_i}{\pi}}\, d\alpha_i \tag{11}$$

Furthermore, from the growth law given by equation (3):

$$dv_i = \frac{\gamma(C-C_e)\alpha_i M}{\rho}\, d\theta \tag{12}$$

or changing the independent variable from time to distance by use of equation (1):

$$dv_i = \frac{\gamma(C-C_e)\alpha_i MAP}{\rho N \rho_p r \pi dRTx}\, dx \tag{13}$$

If dv_i is eliminated between equations (11) and (13), the resulting equation can be integrated between the limits (α_o, x_i) and (α_i, x) to yield:

$$\alpha_i = \left[\int_{x_i}^{x} \frac{\sqrt{\pi}\,\gamma(C-C_e)MdP}{2\rho N \rho_p r RTx}\, dx + \sqrt{\alpha_o} \right]^2 \tag{14}$$

Finally, introducing the accomplishment factor ϕ yields the desired expression for α_i:

$$\alpha_i = \left[Q \int_{x_i}^{x} \frac{1-\phi}{x}\, dx + \sqrt{\alpha_o} \right]^2 \tag{15}$$

where:

$$Q = \frac{\sqrt{\pi}\,\gamma\delta MdP}{2\rho N \rho_p r RT} \tag{16}$$

From equation (2), the number of particles initiated per second over the x interval dx_i is $n_o dx_i$. Therefore, the particle area passing position x per second of all particles initiated over the x interval dx_i is $n_o \alpha_i dx_i$. Then the total surface area of all particles passing position x per second (a_t) is the summation of $n_o \alpha_i dx_i$ for all x_i's less than x, i.e.,

$$a_t = n_o \int_o^x \alpha_i dx_i \tag{17}$$

Equation (17) with the formulation of α_i given by equation (15) is the desired expression for a_t as a function of Φ and x.

The physical problem has now been completely stated mathematically. We turn now to finding a solution of the differential mass blaance, equation (8), which satisfies its boundary condition. This boundary condition is that a_t, the particle area passing position x per second, is zero at x = 0, and is explicitly stated in the integral equation for a_t, equation (17).

C. SOLUTION OF MODEL EQUATIONS

Expanding equation (8) and solving for $d\Phi/dx$ yields:

$$\frac{d\Phi}{dx} = \frac{Fa_t(1-\Phi)}{x^2} - \frac{\Phi}{x} \tag{18}$$

Since by definition, Φ is bounded between 0 and 1, as x gets very large, Φ/x approaches 0, and thus, from equation (18), $d\Phi/dx$ is either 0 or positive since F, a_t, $(1-\Phi)$, and x are all positive quantities. However, as x gets very large, $d\Phi/dx$ cannot remain positive, for then Φ would increase without bound. Thus, a physically meaningful solution of equation (8) must indicate that $d\Phi/dx$ approaches zero as x approaches infinity. This fact suggests that Φ = constant may be a solution to the problem, and this hypothesis is most easily tested by direct substitution.

If equation 18 is solved for a_t assuming Φ is constant, the result is:

$$a_t = \frac{\Phi}{F(1-\Phi)} \, x \tag{19}$$

Thus, if ϕ is indeed constant, a_t is a linear function of x, and equation (17) must also show a_t to be a linear function of x. Performing the integration in equation (15) for ϕ equals constant, we obtain after squaring the bracket:

$$\alpha_i = Q^2(1-\phi)^2\left(\ln \frac{x}{x_i}\right)^2 + 2\sqrt{\alpha_o}\, Q(1-\phi) \ln \frac{x}{x_i} + \alpha_o \qquad (20)$$

If this expression for α_i is substituted into equation (17) and the integration performed, the result is:

$$a_t = \left[2n_o Q^2(1-\phi)^2 + 2n_o\sqrt{\alpha_o}\, Q(1-\phi) + n_o\alpha_o\right] x \qquad (21)$$

again, a linear function of x, and, thus, ϕ = constant is a solution to equation (8). Equating the x coefficients in equations (19) and (21) yields the relation between the accomplishment factor ϕ and the three parameters Fn_o, Q, and α_o:

$$\frac{\phi}{Fn_o} = 2Q^2(1-\phi)^3 + 2\sqrt{\alpha_o}\, Q(1-\phi)^2 + \alpha_o(1-\phi) \qquad (22)$$

The only solution to equation (22) with any physical meaning is the one for ϕ between 0 and 1. This solution is unique since as ϕ is increased from 0 to 1 while the parameters are held constant, the right-hand side of equation (22) decreases monotonically while the left-hand side increases monotonically. Thus, the left and right-hand sides can have only one value in common, and this value will correspond to a unique value of ϕ. Also, it can be shown that a value of ϕ between 0 and 1 which is a solution of equation (22) will always exist for any finite values of the parameters Fn_o, Q, and α_o. As ϕ is increased from 0 to 1, the left-hand side of equation (22) increases from zero to a finite limit while the right-hand side decreases from a finite limit to zero. Since both the left and right-hand sides of equation (22) are continuous functions of ϕ, there will always be some value of ϕ between 0 and 1 for which the left-hand side equals the right-hand side.

Since the differential mass balance, equation (8), together with its boundary condition contained in equation (17), completely specifies a unique physical problem, we can assume that there is only one physically meaningful solution to equation (8). This solution should contain one arbitrary constant the value of which is determined by the boundary condition. Since ϕ = constant is a solution of equation (8), and the value of ϕ is uniquely specified by equation (17), it can be concluded that ϕ = constant is the only physically meaningful solution to equation (8). Furthermore, this solution will always exist as should be required of an equation describing a real physical situation.

D. DERIVATION OF AVERAGE PARTICLE VOLUMES AND THE PARTICLE SIZE DISTRIBUTION

Now that the solution ϕ = constant has been verified, the number and weight average particle sizes and the frequency function for the particle size distribution can be calculated. The number average particle volume is defined as the total particle volume in a representative sample divided by the number of particles in that sample. As a representative sample we take all of the particles leaving the rocket chamber in one second. If L is taken to be the chamber length (cm), then the total particle volume leaving the chamber is:

$$\int_o^L n_o v_i(x_i, L)\, dx_i$$

where $v_i(x_i, L)$ is the volume at $x = L$ of a particle initiated at $x = x_i$. The total number of particles leaving the chamber per second is $n_o L$, and thus the number average particle volume, V_n, is given by:

$$V_n = \frac{\int_o^L n_o v_i(x_i, L)\, dx_i}{n_o L} \tag{23}$$

From equations (10) and (15), $v_i(x_i, L)$ is computed to be:

$$v_i(x_i, L) = \frac{1}{6\sqrt{\pi}} \left[Q(1-\phi) \ln \frac{L}{x_i} + \sqrt{\alpha_o} \right]^3 \tag{24}$$

Cubing the bracket in equation (24) and substituting into equation (23) yields for V_n:

$$V_n = \frac{1}{\sqrt{\pi}} \left[Q^3 (1-\xi)^3 + Q^2(1-\xi)^2 \sqrt{\alpha_o} + \frac{1}{2} \alpha_o Q(1-\xi) + \frac{1}{6}(\alpha_o)^{3/2} \right] \qquad (25)$$

The weight or volume average particle volume, V_v, for a sample of discrete particles is defined as the sum over all particles of the product of the volume fraction times the particle volume. This in turn is equal to the sum over all particles of the square of the volume divided by the total volume, i.e.

$$V_v = \frac{\Sigma n_i v_i^2}{\Sigma n_i v_i} \qquad (26)$$

Generalizing equation (26) for the continuous distribution of particles leaving the rocket chamber yields:

$$V_v = \frac{\int_o^L n_o [v_i(x_i,L)]^2 dx_i}{\int_o^L n_o v_i(x_i,L) dx_i} = \frac{\int_c^L [v_i(x_i,L)]^2 dx_i}{LV_n} \qquad (27)$$

Combining equations (24) and (27) gives the desired formulation for V_v:

$$V_v = \frac{20}{\sqrt{\pi}} Q^3 (1-\xi)^3 + \frac{1}{\pi V_n} \left[\frac{5}{6} Q^2 (1-\xi)^2 \alpha_o^2 + \frac{1}{6} Q(1-\xi)\alpha_o^{5/2} + \frac{1}{36} \alpha_o^3 \right] \qquad (28)$$

The density or frequency function, $f\left(v_i(x_i,L)\right)$, for the particle distribution is defined so that the probability of obtaining a particle between volumes v_1 and v_2 is given by the integral of fdv between the limits v_1 and v_2. This definition requires that the integral of fdv between the limits v_o and infinity to be equal to unity. Define the distribution function, $F_D\left(v_i(x_i,L)\right)$, as the total volume of all particles of volume less than $v_i(x_i,L)$ which pass the position x = L per second. Then:

$$F_D\left(v_i(x_i,L)\right) = \int_{x_i}^L n_o v_i(x_i,L)\, dx_i \qquad (29)$$

Now, from the definition of f, the volume of all particles of volume between v - dv/2 and v + dv/2 is given by $n_o L v f(v) dv$, and thus, $F_D\left(v_i(x_i, L)\right)$ is also given by:

$$F_D(v) = \int_{v_o}^{v} n_o L v f(v) dv \tag{30}$$

where it is understood that v is a function of both x_i and L. Differentiating equation (30) with respect to v and rearranging yields the desired relation between f(v) and $F_D(v)$, namely:

$$f(v) = \frac{F_D'(v)}{n_o L v} \tag{31}$$

From the chain rule:

$$F_D'(v) = \frac{dF(v)}{dx_i} \frac{dx_i}{dv} \tag{32}$$

By differentiating equation (29) with respect to x_i:

$$\frac{dF(v)}{dx_i} = - n_o v \tag{33}$$

By differentiating equation (24) with respect to x_i and applying equation (15):

$$\frac{dv}{dx_i} = \frac{-Q}{2\sqrt{\pi}} \frac{\alpha}{x_i} \tag{34}$$

Substituting equations (33) and (34) into equation (32) and substituting the resulting expression for $F_D'(v)$ into equation (31) yields:

$$f(v) = \frac{2\sqrt{\pi}}{Q(1-\phi)\alpha} \frac{x_i}{L} \tag{35}$$

Finally eliminating x_i/L from equation (35) by means of equation (24) and making use of the geometrical relation between v and α yields the final form of the frequency function:

$$f(v) = \frac{2\pi^{1/6}}{Q(1-\phi)(6v)^{2/3}} \exp\left[\frac{-\pi^{1/6}\left[(6v)^{1/3} - (6v_o)^{1/3}\right]}{Q(1-\phi)}\right] \tag{36}$$

E. DISCUSSION OF MODEL

Examination of the equations for V_n, V_v, and f(v) shows that these three quantities are independent of the chamber length L, and thus the particle size distribution does not vary throughout the entire chamber length. This situation is the result of the residence time distribution of the particles in the chamber. As the chamber length is increased, there will be a larger number of large particles leaving the chamber because of the increased residence time of particles formed at a given distance from the head end of the chamber. However, there will also be a larger number of smaller particles leaving the chamber because the residence time of particles formed at a given distance from the chamber exit will have been reduced because of the increase of gas velocity with increasing x. These two effects of increasing chamber length counterbalance one another to result in a particle size distribution independent of L. Furthermore, it should be noted that the range of particle sizes is independent of L. Particles initiated at x = 0 theoretically have an infinite residence time and thus an infinite volume while particles initiated at x = L have a zero residence time and thus a volume equal to v_o.

Depending upon the origin of the nuclei, the particle size distribution can also be independent of the chamber diameter. If all of the nuclei are formed in the low temperature film adjacent to the propellant surface, then, since n_o is the number of nuclei introduced into the chamber per sec per cm of chamber length, n_o will be proportional to d. Now, if equation (22) is multiplied by Q, it can be written as:

$$\frac{K_1}{K_2}\frac{Q}{n_o} = 2Q^3(1-\Phi)^3 + 2Q^2(1-\Phi)^2\sqrt{\alpha_o} + Q(1-\Phi)\alpha_o \qquad (37)$$

where:

$$K_1 = \frac{\sqrt{\pi}\,\delta M dP}{2\rho N \rho_p rRT} = \frac{Q}{Y} \qquad (38)$$

$$K_2 = \frac{1}{4\pi}\left[\frac{P}{N\rho_p rRT}\right]^2 = \frac{F}{Y} \qquad (39)$$

$$\frac{K_1}{K_2} = \frac{2\pi^{3/2}\,\delta\,MN\rho_p rRT}{P}\,d = \frac{Q}{F} \tag{40}$$

Equation (40) shows K_1/K_2 to be proportional to d, and if n_o is proportional to d, the left-hand side of equation (37) is independent of d. Therefore, the right-hand side of equation (37) is independent of d, and consequently, $Q(1-\delta)$ is independent of d. Since equation (36) shows $f(v)$ to depend only on $Q(1-\delta)$ for a given value of v_o, the particle size distribution is independent of the chamber diameter if n_o is proportional to d.

For the model to be valid, it is not necessary to assume that all of the nuclei are formed in the gas film adjacent to the propellant surface, but merely that n_o be constant. For instance, if nuclei are formed in the main gas stream, then the rate of formation of nuclei per unit volume would have to be constant throughout the entire chamber. However, under these conditions n_o will be proportional to d^2 and thus the particle size distribution will be a function of d.

If it is assumed that the nucleus size is very small, the model equations can be greatly simplified as follows: Divide the right-hand side of equation (37) by $2\sqrt{\pi}$ and then add to it the quantity:

$$\frac{1}{6\sqrt{\pi}}\,\alpha_o^{3/2} = v_o$$

The result is then equal to V_n as given by equation (25). We therefore have:

$$V_n = \frac{1}{2\sqrt{\pi}}\,\frac{K_1}{K_2}\,\frac{\delta}{n_o} + v_o \tag{41}$$

Since both δ and n_o can be varied independently of v_o if γ is allowed to vary, equation (41) indicates that V_n is independent of v_o if v_o is small compared to V_n. Under these conditions, then, the terms containing α_o in equations (25) and (28) can be neglected to give:

$$V_n = \frac{1}{\sqrt{\pi}}\,Q^3(1-\delta)^3,\quad v_o \ll V_n \tag{42}$$

$$V_v = \frac{20}{\sqrt{\pi}} Q^3(1-\epsilon)^3, \quad v_o \ll V_v \tag{43}$$

Then, if equation (42) is solved for $Q(1-\epsilon)$ and the result is substituted into equation (36) while letting v_o approach zero, f(v) becomes:

$$f(v) = \frac{2}{V_n^{1/3}(6v)^{2/3}} \exp\left[-(6v/V_n)^{1/3}\right], \quad v_o \to 0 \tag{44}$$

Making use of equation (41), V_n and V_v can also be written as:

$$V_n = \frac{1}{2\sqrt{\pi}} \frac{K_1}{K_2} \frac{\dot{\epsilon}}{n_o}, \quad v_o \ll V_n \tag{45}$$

$$V_v = \frac{10}{\sqrt{\pi}} \frac{K_1}{K_2} \frac{\dot{\epsilon}}{n_o}, \quad v_o \ll V_v \tag{46}$$

It can be seen that when v_o is small compared to V_n, the ratio of V_v to V_n is 10. This is the maximum value for this ratio since as v_o is increased, it will become significant compared to V_n before affecting V_v. In the limit as v_o gets very large V_v/V_n approaches unity.

The conditions under which V_n will be large compared to v_o are affected by the magnitude of K_1/K_2 and thus the physical significance of this parameter is of interest. A reduced expression for K_1/K_2 is given by equation (40). However, the physical significance is more easily discernable from the following expanded formulation:

$$\frac{1}{2\sqrt{\pi}} \frac{K_1}{K_2} = \frac{M}{\rho} C_i N \rho_p r \sqrt{\pi} d \frac{RT}{P} - \frac{M}{\rho} C_e N \rho_p r \sqrt{\pi} d \frac{RT}{P} \tag{47}$$

The first term on the right-hand side of equation (47) is the condensed volume of gaseous oxide generated per unit length of chamber per second. The second term is the volume of this material which remains in the gas phase at equilibrium. Therefore, $\frac{1}{2\sqrt{\pi}} \frac{K_1}{K_2}$

is the volumetric rate of generation per unit chamber length of oxide that would condense if condensation progressed to equilibrium. If C_e is small compared to C_i, as is generally the case, and we define m and n as:

m = moles of oxide produced upon burning one gram of propellant

n = number of nuclei produced upon burning one gram of propellant

then, from equations (45) and (46) and the assumption that n_o is proportional to d, V_n and V_v are given by:

$$V_n = \frac{Mm}{\rho n}\phi, \qquad C_e \ll C_i,\ v_o \ll V_n \tag{48}$$

$$V_v = 20\frac{Mm}{\rho n}\phi \qquad C_e \ll C_i,\ v_o \ll V_v \tag{49}$$

The value of ϕ will depend upon the values of n_o and the growth constant, γ. For small values of n_o and γ, very little condensation will take place and ϕ will be essentially zero. Under these conditions, varying n_o will not affect $(1-\phi)$ significantly, and thus will not alter the driving force for condensation, so the amount of material that condenses upon a single particle will not be affected by n_o. However, varying the growth constant will affect the growth of a single particle even though it will not affect $(1-\phi)$. Therefore, when ϕ is essentially 0, f(v) will be independent of n_o and depend only upon γ and v_o for fixed values of K_1. Aside from the above physical argument, this conclusion is evident from examination of equation (36).

When ϕ is close to zero there will probably be significant condensation in the rocket nozzle. Thus, although the model will apply to the particle size distribution of the particles as they leave the chamber, it will not be applicable to the particles leaving the nozzle. In order to apply the model to particles leaving the nozzle, ϕ must be essentially unity. Under these conditions all of the condensable oxide will have condensed and the distribution will depend only upon the number of nuclei upon which it has condensed. Thus, as indicated by equations (44), (45), and (46), the particle size

distribution will be independent of γ, and if v_o is essentially zero, the distribution will depend upon only one arbitrary parameter, n_o.

The discussion thus far has been concerned only with particle volumes. Equations for the number average particle diameter, D_n, and the weight or volume average particle diameter, D_v, are now presented without derivation. D_n and D_v are defined by equations (50) and (51).

$$D_n = \frac{\Sigma n_i D_i}{\Sigma n_i} \tag{50}$$

$$D_v = \frac{\Sigma n_i v_i D_i}{\Sigma n_i v_i} \tag{51}$$

For the most general case of the model D_n and D_v are given by:

$$D_n = \frac{1}{\sqrt{\pi}} \left[Q(1-\phi) + \sqrt{\alpha_o} \right] \tag{52}$$

$$D_v = \frac{1}{\sqrt{\pi}} \left[4Q(1-\phi) + \frac{\alpha_o^2}{6Q^3(1-\phi)^3 + 6Q^2(1-\phi)^2\sqrt{\alpha_o} + 3Q(1-\phi)\alpha_o + \alpha_o^{3/2}} \right] \tag{53}$$

For the special case where the nucleus diameter D_o is small compared to D_n, D_n and D_v are given by:

$$D_n = \frac{1}{\sqrt{\pi}} Q(1-\phi) = \frac{1}{\sqrt{\pi}} \left(\frac{1}{2} \frac{K_1}{K_2} \frac{\phi}{n_o} \right)^{1/3} \tag{54}$$

$$D_v = \frac{4}{\sqrt{\pi}} Q(1-\phi) = \frac{4}{\sqrt{\pi}} \left(\frac{1}{2} \frac{K_1}{K_2} \frac{\phi}{n_o} \right)^{1/3} \tag{55}$$

For this case, the ratio of D_v to D_n is equal to 4.

III. COMPARISON OF THE MODEL TO EXPERIMENTAL DATA

The model will be compared to particle size distributions obtained in motor firings conducted by Sehgal* at the Jet Propulsion Laboratory. In his work cylindrically perforated grains were fired into a stainless steel collecting tank and the particle size distribution of the collected aluminum oxide was determined by photomicrographic techniques.

The propellant fired by Sehgal was composed of 12 per cent aluminum, 19 per cent polyurethane binder, and 69 per cent ammonium perchlorate. For this propellant, equilibrium combustion product compositions have been calculated for chamber pressures of 500 and 150 psi. From these calculations the various constants required by the model have been calculated and are listed in Table I.

TABLE I

Physical Parameters for Model

	Chamber Pressure (psi)	
	500	150
P (atm)	34.0	10.2
T (°K)	3413	3279
C_i (moles/cc)	7.99×10^{-6}	2.53×10^{-6}
C_e (moles/cc)	0.936×10^{-6}	0.298×10^{-7}
$\delta = C_i - C_e$	7.90×10^{-6}	2.50×10^{-6}
N (moles/gm)	0.03382	0.03431
M (gm/mole)	101.94	101.94
ρ (gm/cm^3)	3.4	3.4
ρ_p (gm/cm^3)	1.76	1.76
r (cm/sec)	0.508	0.343

* Sehgal, Robert, An Experimental Investigation of a Gas-Particle System, Technical Report No. 32-238, Jet Propulsion Laboratory, Pasadena, Calif. 16 March 1962.

As mentioned in the introduction, the quantities C_i and C_e are actually fictitious and some arbitrary assumption is required for their calculation. The values of C_i in Table I were calculated assuming that all of the aluminum in the propellant is oxidized to Al_2O_3 and that this quantity of Al_2O_3 is initially present in the gas phase. C_e was calculated assuming that all of the aluminum existing in any form in the gas phase at equilibrium exists as Al_2O_3 gas.

The propellant grains fired by Sehgal had an initial port diameter of 2-inches and a web thickness of 3-inches. Thus, during the firings the port diameter increased from 2 to 5-inches. Depending upon the origin of the nuclei, as discussed earlier, this variation in d may or may not affect the particle size distribution. Nevertheless, for the comparison of the model to the data, an average d of 3.75-inches (9.53 cm) has been used.

Samples of the particles collected by Sehgal at chamber pressures of 500 and 150 psi were forwarded to this laboratory. These particles were dispersed and photographed through an electron microscope, and by counting the particles in the photomicrographs particle size distributions were obtained. The particles were spherical so the particle size analysis was relatively simple. For the sample obtained at 500 psi, 2041 particles were counted while at 150 psi the total count was 3180. The resulting particle size averages are listed in Table II. The total particle count at 150 psi was insufficient to obtain a good statistical value of V_v.

TABLE II

Experimental Particle Size Averages

	Pressure (psi)	
	500	150
$V_n(\mu^3)$	0.750	0.0274
$V_v(\mu^3)$	13.5	--
$D_n(\mu)$	0.588	0.185
$D_v(\mu)$	2.39	0.790

(TABLE II CONTINUED)

	Pressure (psi)	
	500	150
V_v/V_n	18.0	--
D_v/D_n	4.07	4.27

From Table II, it is seen that the ratio V_v/V_n at 500 psi is 18.0, within 10 per cent of the theoretical value of 20 predicted by the model when v_o is small compared to V_n. Furthermore, at 500 and 150 psi, values of the ratio D_v/D_n are 4.07 and 4.27, respectively. These values are also within 10 per cent of the predicted value of 4.0. It appears, therefore, that the special case of the model for which v_o is small compared to V_n describes the experimental data very well. The most stringent test of this conclusion is a comparison of the experimental frequency functions to the theoretical frequency functions for this special case. These frequency functions are compared in Figures 3 and 4 for chamber pressures of 500 and 150 psi, respectively. The solid lines were calculated from equation (44) using the experimental values of V_n given in Table II. The individual points on the graphs are experimental. Excellent agreement between the model and the experimental data prevails over nearly five orders of magnitude of both f(v) and v.

On the basis of the excellent agreement between the model and the experimental data it can be concluded that Φ is essentially unity in the chamber, for this is the only case for which the model should apply to the particles leaving the nozzle. Therefore, the particle size distribution is dependent upon only one arbitrary parameter, n_o.

Values for n_o have been calculated from equation (45) using the experimental values for V_n and the parameters for the propellant and firing conditions listed in Table I. These values for n_o are 2.35×10^{12} and 4.48×10^{13} nuclei/sec, cm at chamber pressures of 500 and 150 psi, respectively. Thus, n_o appears to be a strong function of pressure with n_o decreasing as pressure increases. Consequently, it appears that the

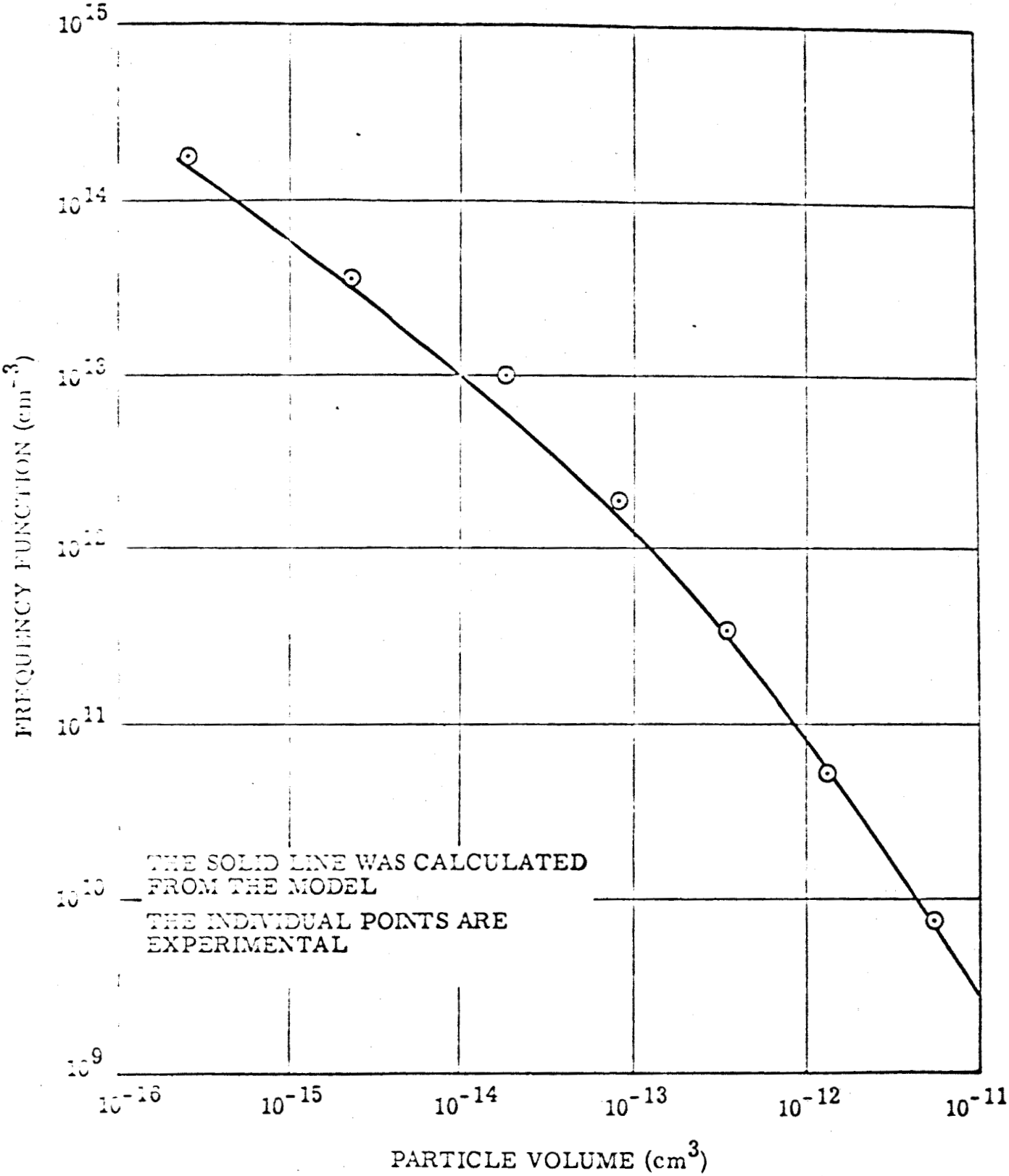

FIGURE 3. THEORETICAL AND EXPERIMENTAL FREQUENCY FUNCTIONS AT A CHAMBER PRESSURE OF 500 PSI.

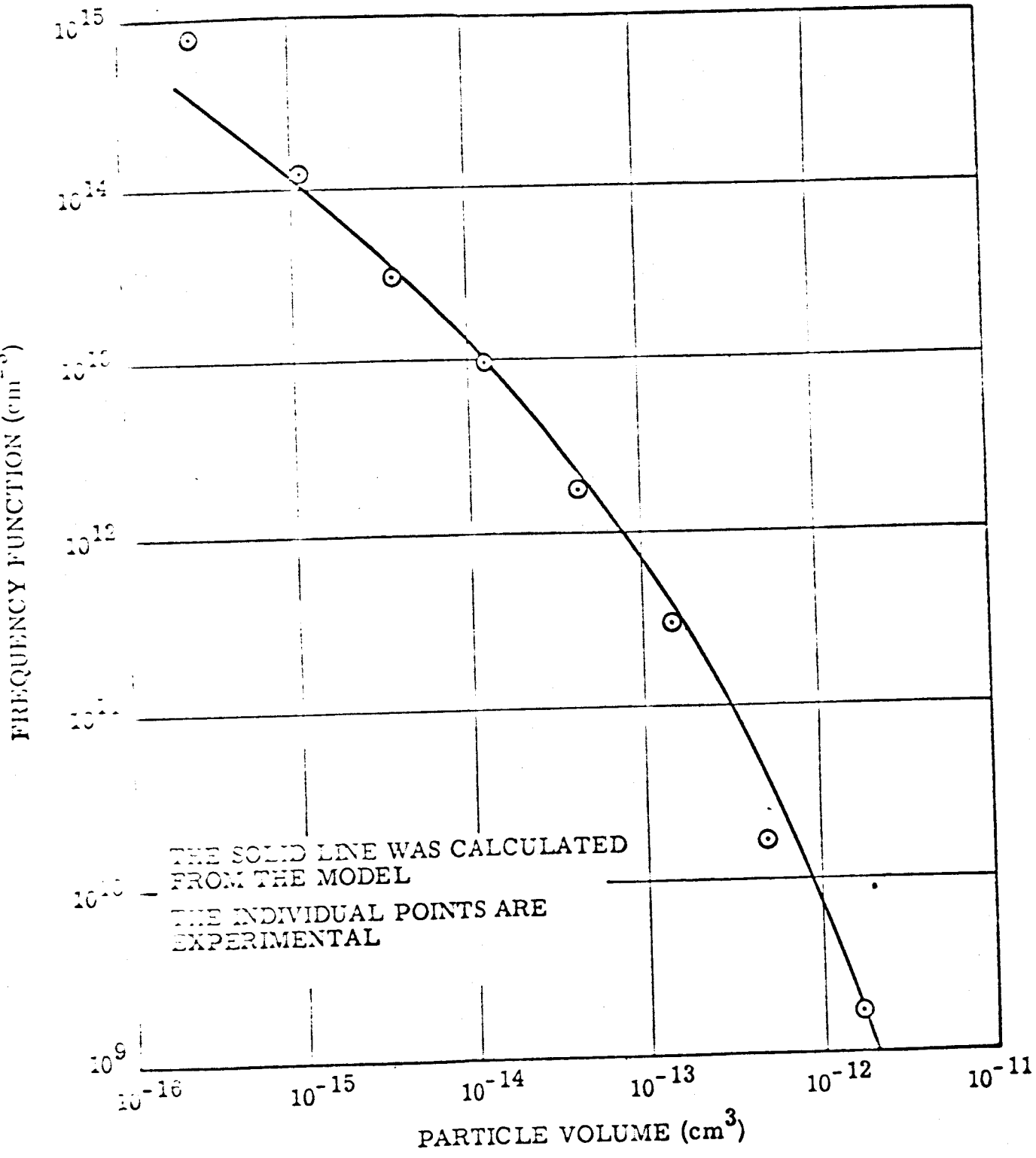

FIGURE 4. THEORETICAL AND EXPERIMENTAL FREQUENCY FUNCTIONS AT A CHAMBER PRESSURE OF 150 PSI

nucleation process is not homogeneous since homegeneous nucleation rates generally increase very rapidly with increasing concentration of the condensable species, and concentration increases with increasing pressure.

The conclusion that the nucleation process is not homogeneous appears quite reasonable since homogeneous nucleation is difficult to achieve in the cleanest of laboratory systems and, therefore, the probability of it occurring in a rocket chamber would appear to be small. Indeed, all of the experimental metal combustion studies as described by Markstein and Christensen, Knipe, and Gordon indicate that prior to ignition, aluminum particles are covered by a thin film of oxide which could, in a finely divided state provide an ample number of heterogeneous nucleation sites. However, exactly how these nuclei are formed from the oxide film is difficult to conceive although the mechanism of formation may be related to the fragmentation of burning aluminum particles observed by Friedman and Macek*.

If the nuclei are formed from the oxide film initially coating the aluminum particles, then, since this oxide film is formed in the low temperature region adjacent to the propellant surface, it seems reasonable to assume that the nuclei are also formed in this region. If this is the case, the particle size distribution will be independent of the chamber diameter, and the relatively large variation of chamber diameter which occurred in Sehgal's firings should have had no effect on the particle size distributions obtained. Furthermore, since from Table I, C_e is small compared to C_i, the simple formulations for V_n and V_v given by equations (48) and (49) should apply with ϕ equal to unity. Consequently:

$$V_n = \frac{Mm}{\rho n} \tag{56}$$

$$V_n = 20\,\frac{Mm}{\rho n} \tag{57}$$

---

* Friedman, R., and A. Macek, "Combustion Studies of Single Aluminum Particles," Ninth International Symposium on Combustion, Academic Press, New York, 1963. p 703.

and the particle size distribution to a first approximation should depend only upon the amount of aluminum in the propellant and the number of nuclei formed per gram of propellant. However, even if the above assumptions are correct, n will still be an unknown parameter of the model which must be determined experimentally.

IV. CONCLUSIONS

1. Agreement is obtained between the experimental data and the particle size distributions predicted by the model. The agreement extends over nearly five orders of magnitude of frequency function and particle volume.

2. The particle size distribution for internal burning, cylindrically perforated, aluminized grains is independent of chamber length and possibly chamber diameter, and depends upon only one arbitrary parameter, n_o. In terms of the number average particle volume, V_n, the frequency function for the particle size distribution is given by:

$$f(v) = \frac{2}{V_n^{1/3}(6v)^{2/3}} \exp\left[-(6v/V_n)^{1/3}\right]$$

3. The agreement between the model and experiment implies that condensation progresses essentially to equilibrium in the rocket chamber.

4. The nucleation mechanism is not homogeneous for aluminized propellant grains.

Acknowledgements: The theoretical analysis was prepared for the Department of the Navy, Bureau of Naval Weapons under Contract No. NOw-61-0687-c and sponsored by the Advanced Research Projects Agency, ARPA Order No. 22-61. The experimental particle size analysis was sponsored by the Jet Propulsion Laboratory under Contract No. 950227.